Report No. FAA-RD-72-94

BOEING 727-100
SAFE BOMB LOCATION STUDY

The Boeing Company
P.O. Box 3707
Seattle, Washington 98124

for

FEDERAL AVIATION ADMINISTRATION
National Aviation Facilities Experimental Center
Atlantic City, New Jersey 08405

NOVEMBER 1972

FINAL REPORT

Prepared for
DEPARTMENT OF TRANSPORTATION
FEDERAL AVIATION ADMINISTRATION
Systems Research & Development Service
Washington, D.C. 20591

TECHNICAL REPORT STANDARD TITLE PAGE

1. Report No.	2. Government Accession No.	3. Recipient's Catalog No.
FAA-RD-72-94		

4. Title and Subtitle	5. Report Date
SAFE BOMB LOCATION	NOVEMBER 1972
	6. Performing Organization Code

7. Author(s)	8. Performing Organization Report No.
Jack Avery Chris Gunther Bob Bistrow Jag Hajari Al Opsahl	FAA-NA-72-91

9. Performing Organization Name and Address	10. Work Unit No.
THE BOEING COMPANY P. O. Box 3707 Seattle, Washington 98124	11. Contract or Grant No. DOT-FA72NA-706
	13. Type of Report and Period Covered FINAL REPORT MAY - SEPTEMBER 1972
12. Sponsoring Agency Name and Address FEDERAL AVIATION ADMINISTRATION Systems Research and Development Service Washington, D. C. 20591	14. Sponsoring Agency Code

15. Supplementary Notes

16. Abstract

This report covers an analytical study to determine the optimum location on a 727-100 airplane for positioning a discovered explosive device. The study consisted of (1) A review of existing methods for predicting blast effects on typical aircraft structure, (2) Selecting candidate locations for analysis, (3) Determining minimum and maximum hole sizes resulting from detonation of a given amount of explosive at the candidate locations, (4) Determining the aircraft's capability for continued safe flight with minimum and maximum holes at the candidate locations and (5) Developing procedures which would provide the best chance of a safe landing in the event of detonation. The study concludes that a location adjacent to the mid-galley door would be the optimum location, that the aircraft would survive with the minimum hole size at any of the three locations and that the maximum hole size would be catastrophic at all but the mid galley door location where, under conditions of limited air speed and gust velocity, continued flight and landing could be effected.

17. Key Words	18. Distribution Statement
BLAST LOADING MECHANICAL RESPONSE EQUIVALENT STATIC LOAD EMERGENCY PROCEDURES SAFE BOMB LOCATION	Approved for U.S. Government only. Transmittal of this document outside the U.S. Government must have prior approval of the Federal Aviation Administration, Systems Research and Development Service.

19. Security Classif. (of this report)	20. Security Classif. (of this page)	21. No. of Pages	22. Price
Unclassified	Unclassified	61	

Form DOT F 1700.7 (8-69)

PREFACE

This report was prepared by The Boeing Company under Department of Transportation Contract DOT-FA72NA-706 and covers work performed during June and July of 1972 by J. V. Hajari of the Structures Design Development Group, Commercial Airplane Group, by C. K. Gunther of the Stress Methods and Allowables Group, Commercial Airplane Group, and by J. G. Avery and R. J. Bristow of the Damage Mechanisms Group, Aerospace Group.

CONTENTS

ILLUSTRATIONS

TABLES

1.0 INTRODUCTION

1.1 General

Today's social climate has imposed conditions on air transport operations which were not anticipated when the present generation of aircraft were conceived. The manifestation of these conditions, reflected by numerous hi-jacking and extortion attempts, is not likely to subside in the forseeable future. Therefore, it is encumbent on all those associated with air transport - airlines, aircraft manufacturers, and regulatory agencies alike - to seek ways to reduce, if not eliminate, this threat to the future of air transport and its users. The Department of Transportation is pursuing an extensive program to deal with this threat through improved pre-boarding screening of passengers and baggage, the use of sky marshals, the development of in-flight disposal of lethal objects and investigation into the on-board bomb containment capability of present aircraft types. It is the latter aspect to which the study reported here is addressed.

1.2 Objective

The objective of this study was to determine the optimum location within a 727-100 aircraft that an explosive device could be placed with the least damage to the structure, aircraft systems and occupants should the device detonate while the aircraft is in flight.

1.3 Assumptions

The following assumptions were made for purposes of this study.

1. The airplane would be a 727-100 in a common airline mixed class configuration.

2. The explosive device would consist of four pounds of 40% nitroglycerine-based commercial dynamite.

3. The explosive device would not detonate until the airplane was depressurized and the device secured at the optimum location.

4. No special bomb handling or suppression equipment would be on board the aircraft.

1.4 Approach

The approach taken for conduct of this study was as follows:

1. Collect and review existing data relating to the effects of explosive detonation on aircraft structure.

2. Select candidate locations considering structural strength margin, systems vulnerability and passenger shielding.

3. Conduct analysis to predict minimum and maximum hole size created by detonation.

4. Conduct analysis to determine aircraft ability for continued flight with minimum and maximum size holes in structure at candidate locations.

5. Select optimum location from results of Step 4 and develop recommended procedures for aircraft operation.

2.0 DATA REVIEW

A review of existing methods and data for predicting the effects of small bomb detonations within the fuselage of airplanes is given in the following paragraphs.

2.1 Scope of Problem

Small bomb detonations within transport-type airplanes produce massive structural damage in the vicinity of the bomb. In order to predict the extent of this damage, methods are required for establishing:

1. The pressure loadings produced by the detonation, including the peak pressure, the total impulse and the pulse duration. These must be known as functions of distance from the blast.

2. The mechanical response of the structure to large, transient pressure loadings. The effect of the blast is to produce large elastic/plastic deformations combined with fracture and tearing.

3. The allowables for the structure under dynamic, large deflection loading conditions.

2.1.1 Blast Loadings - No experimental data is on-hand for the blast loadings produced by 4 lbs. of 40% commercial dynamite as a function of distance from the blast. However, Reference 1 defines this quantity of dynamite as the equivalent of 3.2 lbs. of TNT. Tables are available, References 2 and 3 for example, giving the resultant pressure loadings for this quantity and type of explosive. The data includes peak overpressure, particle velocities, mach number, reflected overpressures, pulse time duration and decay parameter.

2.1.2 Mechanical Response - There are no verified methods, as such, for predicting the local response of airplane structure to internal blasts. The recognition of this fact by the Air

2.1.2 Mechanical Response (cont'd)

Force has led to the recent funding of research in this area, for example AF Contract F33615-72-Q-1045, "Effects of Internal Blast on Combat Aircraft Structures". The results of this program are not yet available.

Computer programs are being developed for handling large deflection, dynamic elastic/plastic response of structure. Boeing is currently completing such a program, Reference 4, using the finite-element method. However, this program does not, as yet, have the capability for handling the fracture and skin-tearing portion of the problem. Based on an evaluation of current computer program technology for blast analysis, this program is the most advanced available. However, because of the fracture development mentioned above and the limitations of this study, the use of this or any other structural analysis computer program is not feasible.

Analysis methods based on rigid-plastic analysis have been used for the blast response of beams, plates and shells (References 5, 6, for example). These methods are useful for predicting plastic deformation, but do not have fracture capability. Simply evaluated relations are available for circular plates and beams; however, the analysis becomes far more complex for the structural shapes required for realistic modeling of aircraft structure. For these reasons, it was felt that the rigid-plastic approach was not suitable for this study.

An energy approach has been described in Reference 7 and 8. In this approach, the blast energy input to the structure is equated to the plastic work done during deformation. The utility of the method depends on a description of the primary mode of deformation and this is not available for complex structure under transient loading. Consequently, this method cannot be used directly on a limited scope program.

2.1.2 Mechanical Response (cont'd)

Of the available analysis methods, the most suitable for this study is an adaptation of the "equivalent static load" (ESL) method. This method is currently in use by the Air Force and other services (Reference 9, for example) for predicting threshold levels of structural failure to blast. The essentials of the method are also outlined in Reference 3, 10, and other sources.

The analysis method consists of estimating a static pressure loading that will do the same amount of damage as the dynamic blast loads. The estimate is based on calculating the response of a one-degree of freedom structural system to the given blast load. This calculation can be done very easily. The equivalent static load can then be computed for components of the airplane structure (e.g., skin, frames, stringers), based on the natural frequency of these components. The components can then be analyzed as for static loading.

The use of this method will provide a rationale for estimating the "hole size" produced by the internal bomb explosion. However, it has to be recognized that this method cannot account for the many unknown aspects of the hole formation problem, nor can any analytical method available.

2.1.3 Structural Allowables - Although design and ultimate strength allowables are available for the airplane loaded under flight conditions, there is little or no data on-hand regarding ultimate strength of components under blast loadings. This area will remain a source of uncertainty.

2.1.4 Empirical Methods - Empirical methods for estimating the response of airplane structure to blast would be ideally suited for this study; however, the available data is not comprehensive enough to provide the complete solution.

The most suitable data on-hand is that summarized in Reference 11. These results are based on tests involving placing charges of TNT inside airplanes of various sizes and estimating the charge levels that would result in 75% probability of structural kill. The test vehicles were all of semi-monocoque construction, and the tests resulted in a correlation between fuselage size and skin thickness, and the charge size required for catastrophic structural damage. These results will be used for confirmation, if possible.

An additional semi-empirical method is given in Reference 12, however, the experimental results and conditions are not specified. This method defines critical values for peak pressure, impulse and pulse duration for threshold damage conditions.

arrangements, and systems routing was made prior to selecting candidate locations. Passenger relocation, shielding provided by passenger accommodations equipment, minimum damage to structure and vital systems were the primary factors considered in selecting candidate locations.

3.1 General Description

Figure 3-1 shows a typical interior arrangement of a 727-100 airplane. The most common configuration is a mixed class with approximately 12 first class and 96 tourist class seats, although other configurations such as single class (up to 131 passengers); all cargo and mixed cargo/passenger are sometimes used. Figure 3-2 and Figure 3-3 show body frame station and major fuselage component diagrams.

There are four electrical raceways in the right hand side upper lobe of the airplane. Two raceways T-1 and T-2 are in crown area close to the centerline of the airplane. Raceway T-1 has wires for Engine No. 2 and autopilot operation and T-2 has wires for Engine No.3 and galley power operation. Raceway R, just above the hatrack, operates all the sidewall lighting and aft cargo compartment lighting and accessories. Raceway HH-3 through the floor beam (See Figure 3-4) has engine No. 3 power feeders. Except for Raceway R, all other raceways are considered essential.

Below the passenger floor are forward and aft cargo compartment, air conditioning bay, and electrical/electronics bay in the forward compartment. All control cables run through the floor beams as shown in Figure 3-4. The 727-100 uses two independent systems (A and B) to hydraulically power the flight controls for all three axes with automatic reversion to manual control provided for the ailerons and elevators.

The fuel tanks are contained entirely within the wing inter-spar section in three main tanks. The fuel tanks are of integral composition, except the one in the wing center section which is within the airplane body, and is made up of bladder cells.

INBOARD PROFILE

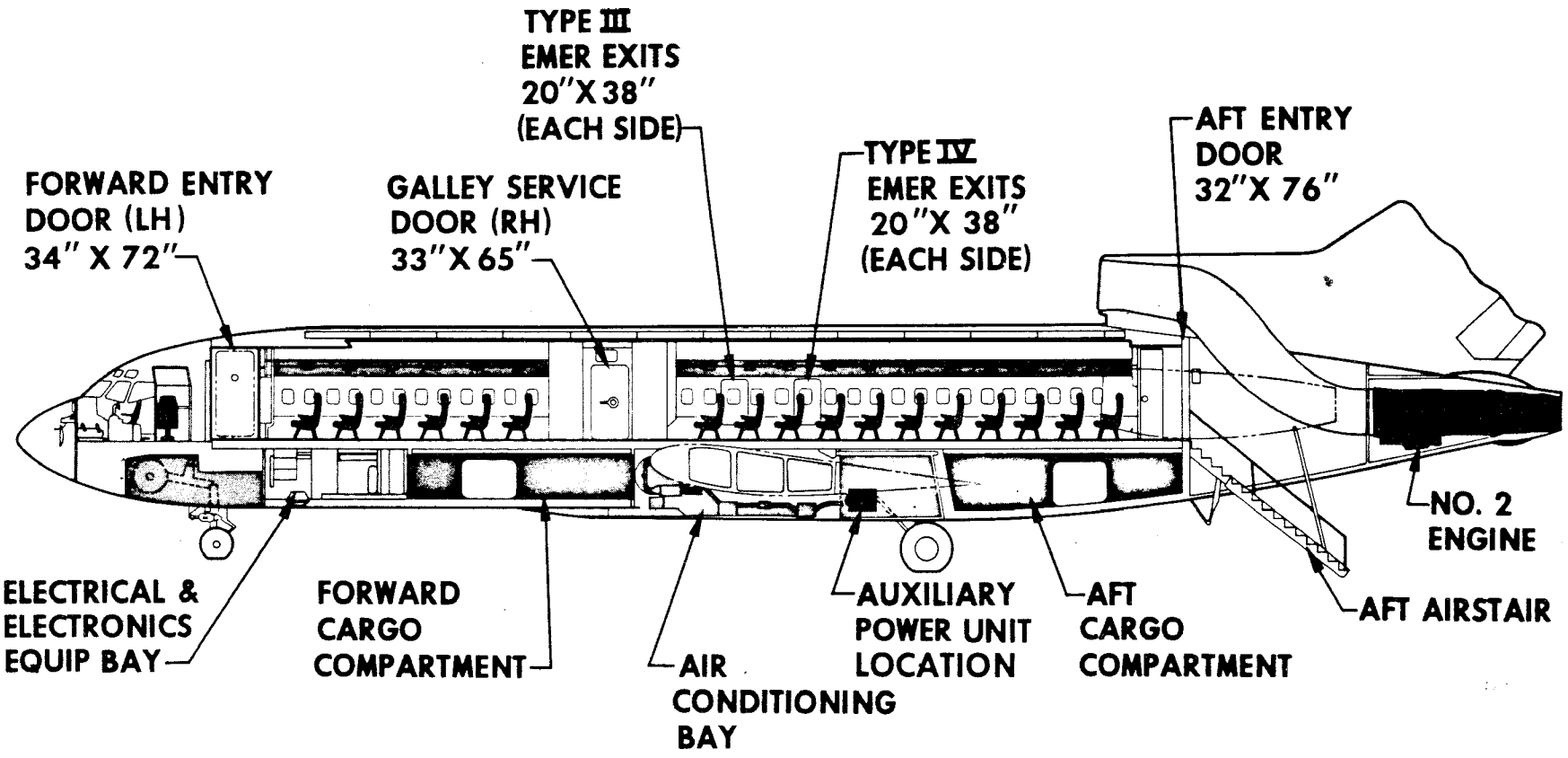

FIGURE 3-1 Inboard Profile

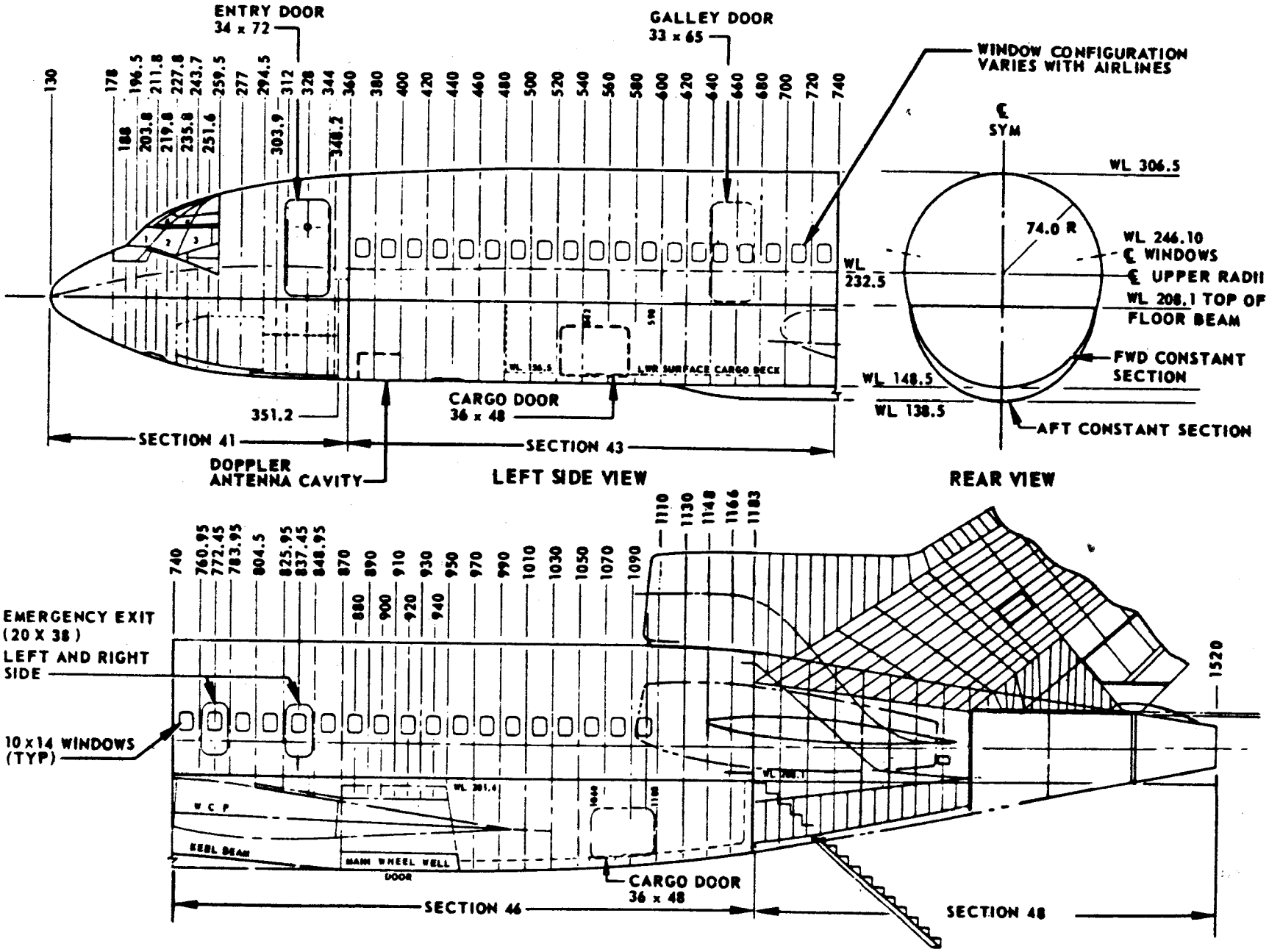

FIGURE 3-2 Body Station Diagram

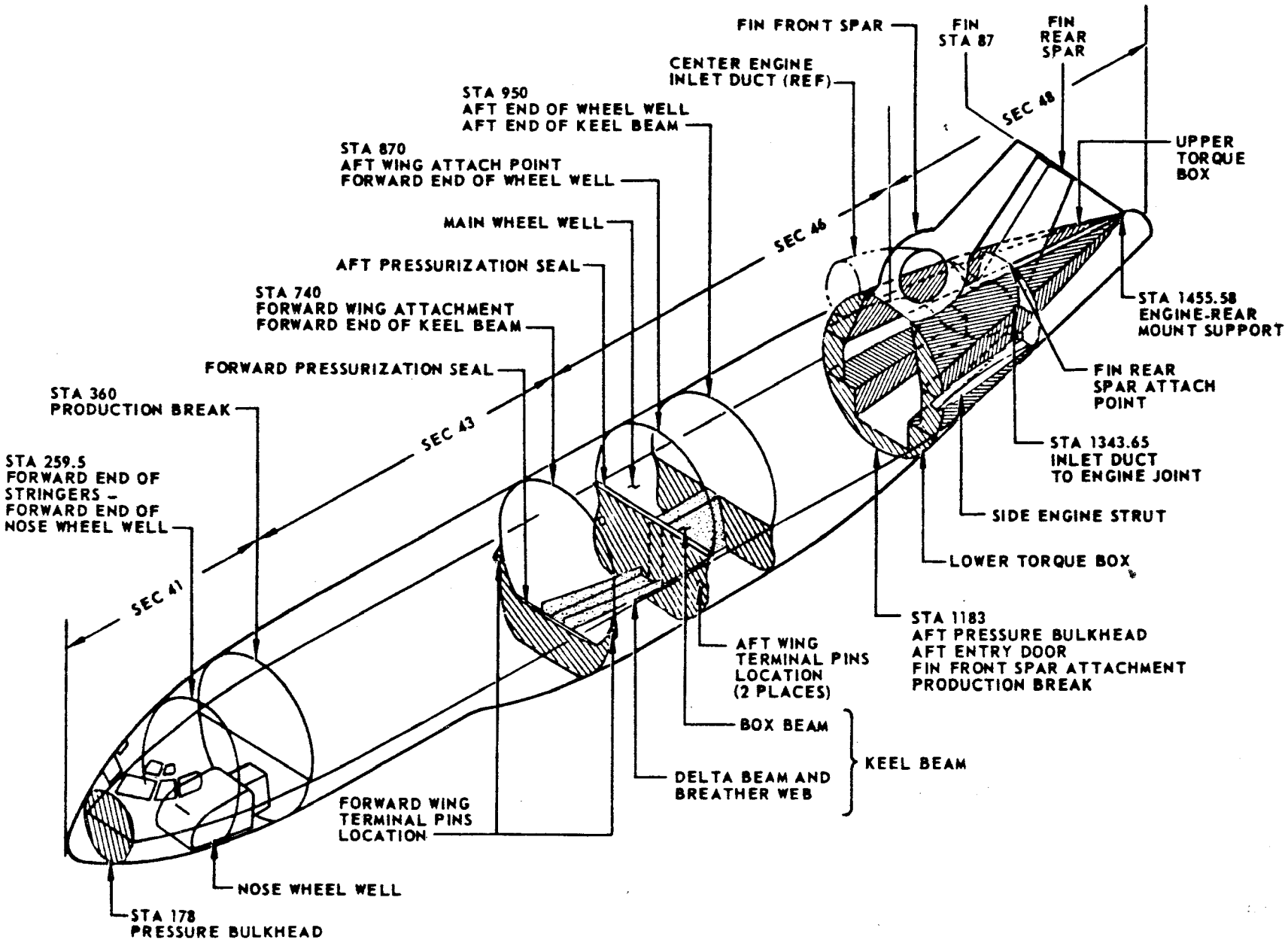

FIGURE 3-3 Major Fuselage Components

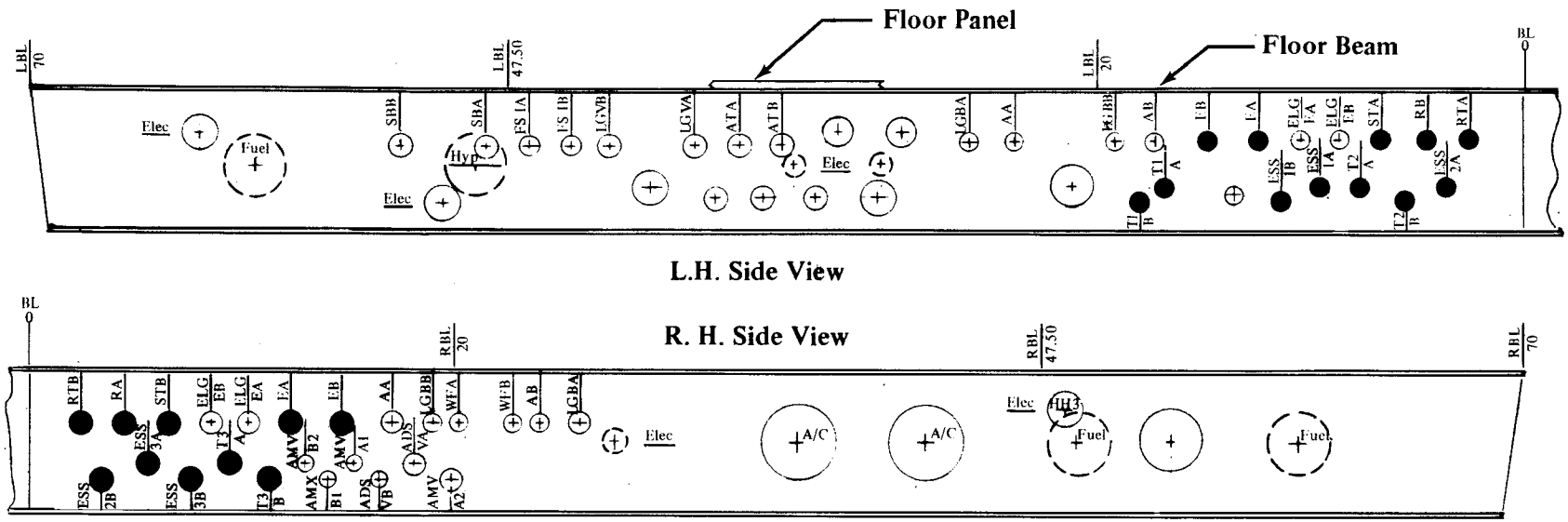

FIGURE 3-4 Systems Run Through Floor Beams

LGBA & B	– Landing Gear Brake
WFA & B	– Wing Flap
AA & B	– Aileron
ADSVA & VB	– Air Distribution Selection Valve
AMV A1, A2, B1, B2	– Air Mixing Valve-Crew, Pass.
SBA & B	– Speed Brake
ELG EA & EB	– Emergency Landing Gear Extension
FS1A & 1B	– Flap Stabilizer Interconnect
LG VB & VA	– Landing Gear Valve
ATA & B	– Aileron Tab
A/C	– Air Conditioning System

● Runs thru Section 43 & 46
⊕ Runs thru Section 43 Only
(+) Runs thru Section 46 Only
EA, EB – Elevator Control
STA, STB – Stabilizer Trim
RA, RB, RTA, RTB – Rudder Control
ESS 1, 2, 3 (A & B) – Engine Start System
T1, 2, 3 (A & B) – Engine Throttle

3.1 General Description (cont'd)

Three fuel system plumbing lines run from rear spar, through Section 46 floor beams to individual engines.

3.2 Location Selection

After a thorough review of aircraft structure, structure loads, interior arrangements and systems (control, electrical, fuel) routing, three candidate locations were chosen as shown in Figure 3-5. The rationale for choosing these locations is as follows:

1. Body Station 500, right hand side, on outboard seat in first class compartment (See Figure 3-6)

   This location was chosen because of (1) the large margin of structure in the forward fuselage in the unpressurized condition, (2) the absence of vital systems under the floor on the right hand side and (3) the shielding provided the rest of passenger cabin and crew compartment by galley, lavatory and partitions.

2. Body Station 660, right hand side on mid-galley door escape slide bustle (See Figure 3-7)

   This location is considered a prime candidate because of (1) the large reinforced cutout already existing because of the door, (2) the ability to partially open the door to facilitate blow out (3) the shielding provided by galley structure and partitions and (4) the absence of vital systems under the floor on the right hand side.

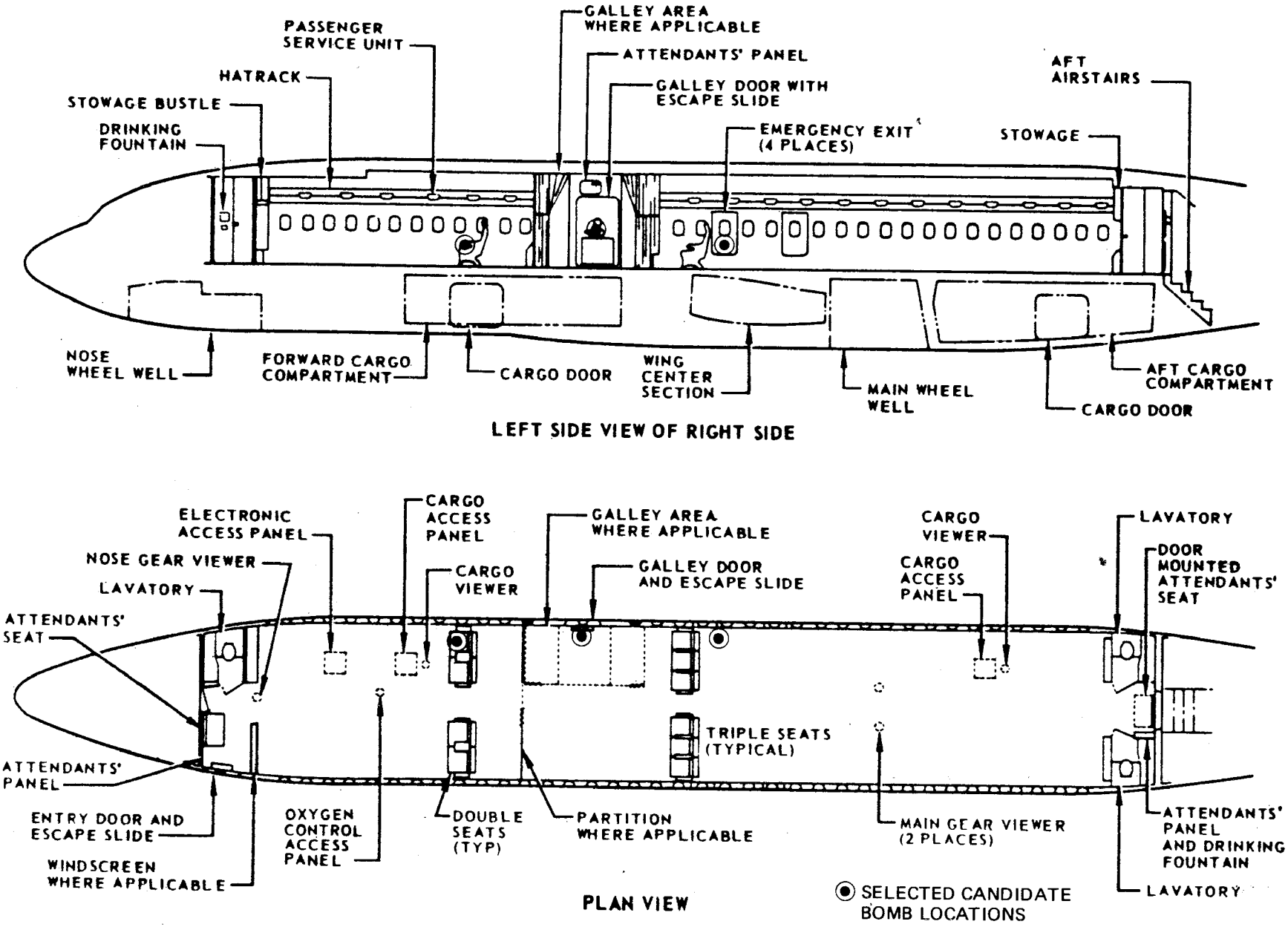

FIGURE 3-5 Passenger Cabin

FIGURE 3-6. STA 500 LOCATION

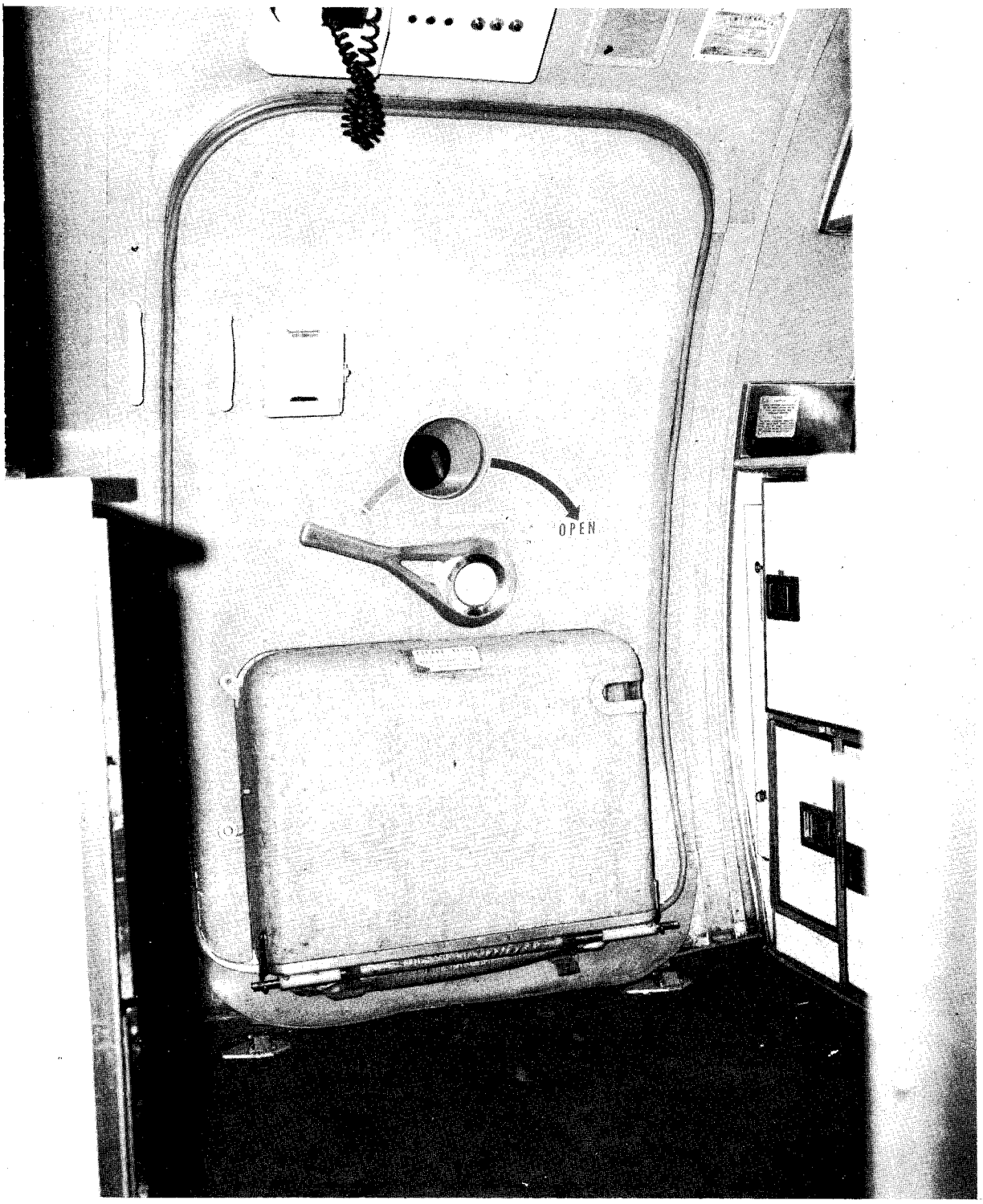

FIGURE 3-7. MID-GALLEY DOOR LOCATION

3.2 Location Selection (cont'd)

3. Body Station 772, right hand side, on the outboard seat adjacent to the opened forward escape hatch. (See Figure 3-8)

This location was included for consideration because of the possibility of providing a large, well reinforced clear opening. It has the disadvantages of fuel cells in the wing center section and lack of shielding for the largest part of the cabin.

Several other locations were considered but dropped for various reasons. A forward cargo compartment was not pursued because seats would have to be moved to gain access (See Figure 3-9) and structural damage would likely extend into critical body bending area. All left hand locations were judged to be unsuitable because of vital control system cables under the floor on that side. All aft body locations were likewise judged to be unsuitable because of fuel lines in the floor structure on both sides. A ventral stair location was not considered because of the likelihood of deactivating the stair during flight.

FIGURE 3-8. EMERGENCY ESCAPE HATCH LOCATION

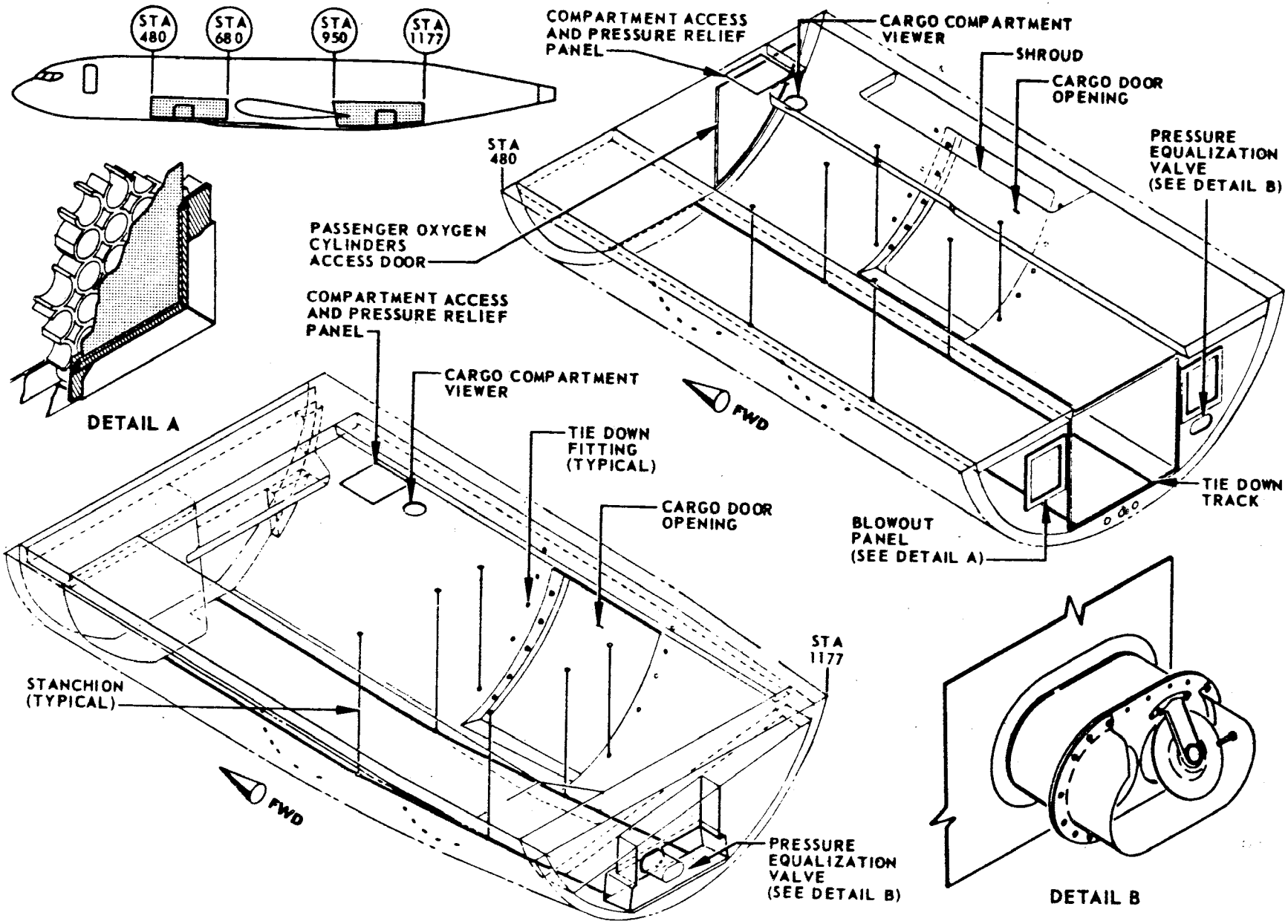

FIGURE 3-9 Cargo Compartments

4.0 DETERMINATION OF STRUCTURAL DAMAGE

4.1 Scope of Problem

The objective of this task is to estimate the size of the structural damage caused by the bomb detonation. This estimate is then used to determine the capability of the remaining structure to carry flight loads.

The estimation of structural damage proceeds in two steps:

a. Estimate the overpressure loadings acting on the structure at various distances from the detonation.

b. Estimate the response of the structure to the dynamic overpressure loadings, including an estimation of structural failure.

Although estimating threshold levels for structural failure under blast loading conditions is a problem that is fairly routine in vulnerability analysis, estimating the size of the damage is not a routine problem, and is normally considered intractable without supporting experimental data for the specific explosive and structure considered.

The reason for this is that the confidence level for predictions of blast pressure loadings and structural response is low. Reference 13 concludes that the state of predictability of blast loading is a factor of 2 on peak pressures and a factor of 4 on loading time duration.

The difficulty in predicting damage size, even when the loads are accurately known, is a difficult problem under static loading conditions, and the difficulty is compounded under dynamic loadings.

For these reasons, the hole size predictions described in the following sections must be regarded as engineering guesses. Computer analysis using a dynamic elastic/plastic code, combined with some experimental data, could improve the confidence of the predictions, but was not within the scope of this program.

4.2 Estimation of Blast Loadings

The 4 pounds of dynamite were assumed to be equivalent to 3.2 pounds of TNT, in accordance with the information reported in Reference 1. The pressure loadings for TNT are tabulated in many sources, and loadings for this study were extracted from Reference 3.

4.2.1 Types of Pressure Loadings - The detonation of the bomb causes a shock wave that travels radially outward from the center of detonation. The shock wave travels at the local speed of sound and results in a rapid increase and decay of pressure.

The blast pressure loadings are characterized by a peak overpressure, a time duration, a decay shape and a total impulse. In addition, the intensity and character of the blast loading changes with distance from the detonation.

As the shock wave travels through the air, the overpressure is not direction dependant. That is, the overpressure represents the pressure that exists at a point in space. This free-air overpressure is called side-on overpressure. The side-on overpressure can be obtained directly from available tabulations.

When the shock wave strikes a structure, however, the pressure loading felt by the structure will be either the reflected overpressure or the Mach stem overpressure, as determined by the angle of incidence between the shock front and the structure.

For nearly "head-on" incidence, the incoming shock wave is reflected from the surface of the structure and the superposition of the incident and reflected waves causes a pressure amplification on the surface. This amplified pressure is the reflected overpressure.

As the angle of incidence is increased, however, a point is reached such that the incident wave does not reflect, but instead travels along the surface, forming a "Mach stem". The pressure loading behind the Mach stem is the Mach stem overpressure, and acts directly on the structure.

In order to simplify loading analysis, it is common practice to transform the actual pressure pulse, which has an exponential decay, into an equivalent triangular shaped pulse having the same total impulse as the actual pulse. This can be done using the "decay parameter," a value that is also available on tabulations.

4.2.2 Magnitude of Pressure Loadings - Magnitudes of relevant blast loading parameters for 3.2 lbs. of TNT are shown in Table 4-1, in terms of radial distance from the detonation. These values were obtained from Reference 3, for a spherical charge.

TABLE 4-1 BLAST LOADING PARAMETERS (3.2 lbs. TNT)

(1) Actual Distance D_a (ft.)	(2) Mach Number	(3) Peak Side-on Over-pressure (PSI)	(4) Reflected Overpres-sure P_r (PSI)	(5) Time Duration (ms)	(6) Decay Parameter α	(7) $\frac{I}{I\Delta}$	(8) β for Mach stem for-mation	(9) Total Impulse Based on Re-flected Over-pressure (psi-ms)	(10) Equiv. Triangular Pulse (based on $P_{reflected}$)	
									P_{max}	t_d
.585	12.80	2,820	21,700	0.29	--	--	39	--	--	0.29
1.76	5.57	515	3,600	0.07	--	--	39	--		0.07
2.93	3.60	206	1,229	0.66	4.5	.365	39	148	448	0.66
4.10	2.61	100	496	0.76	2.8	.475	39	89.6	235	0.76
5.26	2.02	53	214	0.97	1.7	.620	39	64.4	133	0.97
6.44	1.67	31	105	1.19	1.2	.700	39	43.7	73.5	1.19
7.60	1.46	19	56	1.41	1.0	.730	39	28.8	40.8	1.41
8.77	1.35	14	38	1.61	0.9	.775	42	23.7	29.4	1.61
9.95	1.29	11	28.4	1.79	0.9	.775	43	19.7	22.0	1.79
11.10	1.24	9	22.9	1.95	0.9	.775	47	17.3	17.7	1.95

Explanation:

(1) Distance from detonation.

(2) The Mach number of the shock front.

(3) Peak side-on overpressure.

(4) Reflected overpressure.

(5) The time duration of the positive phase of the pressure pulse.

(6) Decay parameter.

(7) This ratio gives the ratio of the actual impulse to the impulse of a triangular pulse.

(8) β is the incidence angle causing formation of a Mach stem.

(9) Total impulse.

(10) These values define the equivalent triangular pulse that has the same impulse and time duration as the actual pulse.

In obtaining these values, several well known scaling parameters were used that correlate the effects of explosions produced by different charge weights. These scaling parameters are specified below:

a. Intensity of Overpressure

$$D_s = \frac{(\rho/\rho_o)^{\frac{1}{3}} D_a}{(W/W_o)^{\frac{1}{3}}} = \frac{f_d}{\lambda} D_a$$

$f_d = (\rho/\rho_o)^{\frac{1}{3}}$ = density transmission factor

$\lambda = (W/W_o)^{\frac{1}{3}}$ = yield factor

D_s = scaled distance, i.e., distance from W_o # having the same intensity as distance D_a from W.#

ρ = air density

ρ_o = air density for reference explosion

D_a = actual distance, i.e., distance from W #

W = weight of explosive

W_o = weight of reference explosive

The density transmission factor is shown in Figure 4-1 as a function of cabin pressure. For the conditions of this study $f_d \approx 1$.

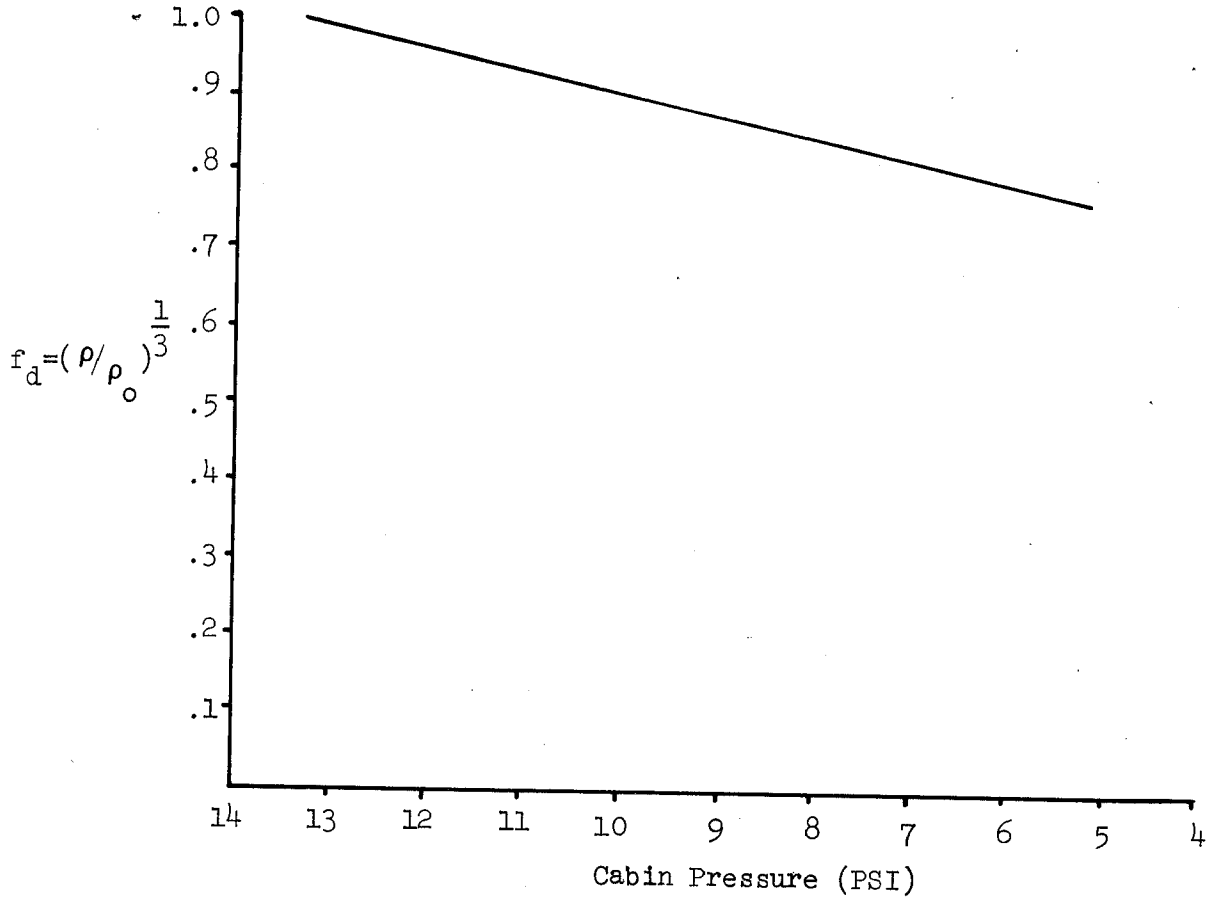

FIGURE 4-1 Density transmission factor

b. Time Scaling

$$T_a = \frac{\lambda T_s}{f_d f_a},$$

T_a = actual time

T_s = scaled time

f_d = density transmission factor

f_a = transmission factor for velocity of sound

This scaling relation applies for both time of arrival and positive pulse duration. For this study:

$$f_d = f_a \approx 1$$

The actual pulse shape was transformed into an equivalent triangular pulse having the same total impulse and time duration. The peak pressure, impulse and time durations for the equivalent triangular pulse are shown graphically in Figure 4-2.

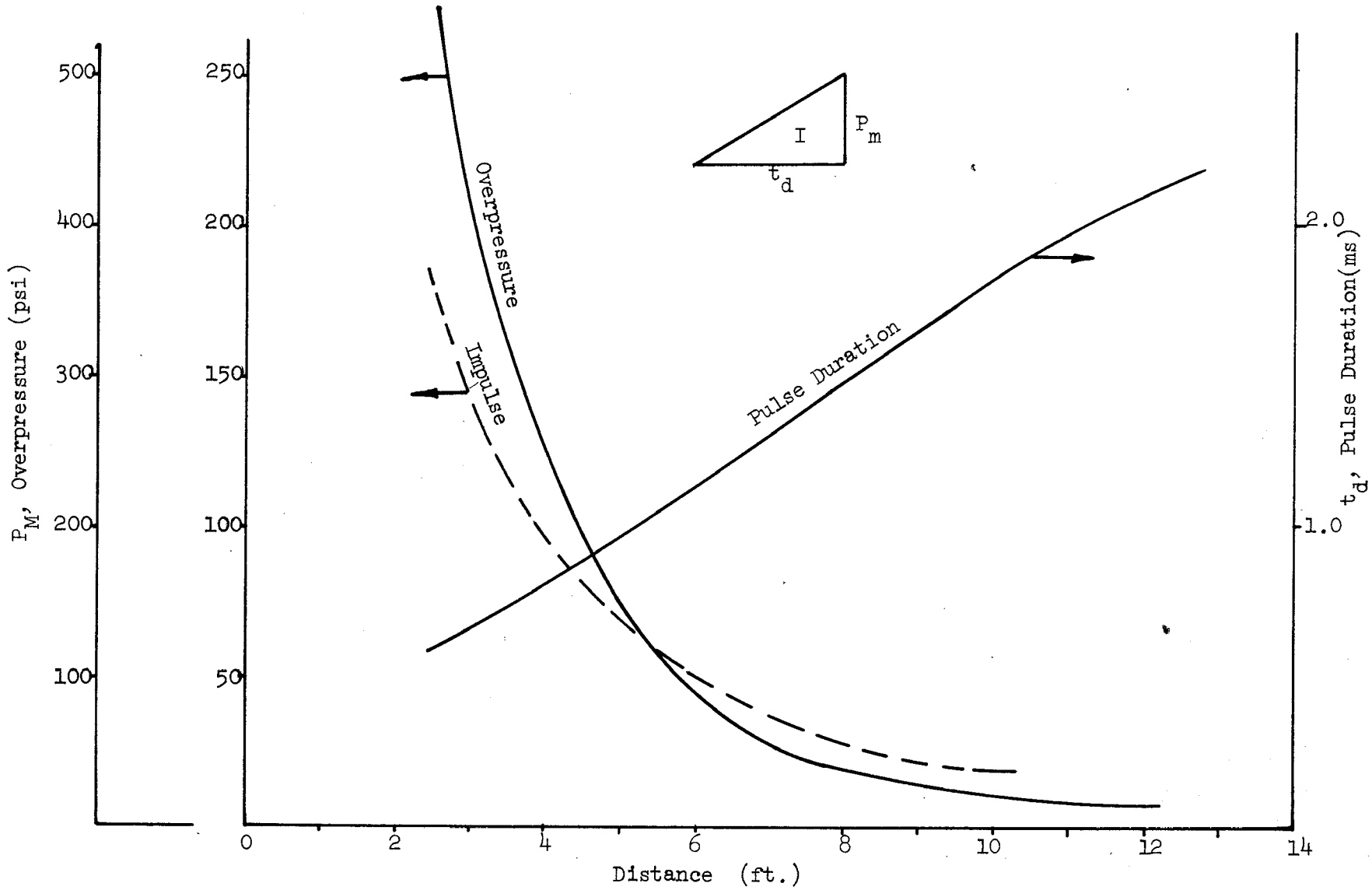

FIGURE 4-2. Equivalent Triangular Pulse

4.3 Estimates of Structural Damage

The estimations of structural damage were made using the following steps:

1. Place the detonation center at the selected location.

2. Calculate the pressure pulse acting on interior points of the fuselage using the methods described in the previous section, including the determination of Mach stem formation.

3. Convert the dynamic pressure loadings to "equivalent" static loads, using the "ESL" technique frequently used in vulnerability analysis for predicting structural failure due to blast.

4. Failure was assumed to occur when the equivalent static pressure load exceeded the ultimate strength capability of skin panels.

Because of the prediction uncertainties mentioned previously, it was decided to establish probable maximum and minimum damage sizes. The damage estimated by using the above procedure was taken to be a maximum, since there was no allowance made for the energy absorption capability of interior padding, seats, hat rack structure, pillows or blankets.

Determination of the suppression effects of these energy absorbing items was beyond the scope of this analysis. Since peak pressures can only be estimated within a factor of 2, as discussed in Section 4.1, it was decided that a rational minimum damage size would be one-half that predicted for the maximum. This assumption, combined with engineering judgement, was used for this study.

The remainder of this section describes the damage estimation procedure in more detail, and gives specific examples from the actual calculations for illustration.

4.3.1 Pressure Pulse Calculations - Reflected and Mach stem overpressures were calculated around the periphery of the fuselage (within a plane passing thru the station location perpendicular to the longitudinal axis of the fuselage), and along the fuselage in the fore and aft directions at an elevation corresponding to the bomb location. It was decided that these calculations would provide adequate insight into the pressure profiles.

The procedure consists of drawing a ray from the detonation and measuring the angle between this ray and a tangent to the fuselage contour at the point of intersection. This angle is the incidence angle, β, between the shock front and the structure.

Critical values of β were tabulated previously in Table 4-1. When β exceeds the critical value, a Mach stem will be formed. When β is less than the critical value the reflected overpressure is used for the structural damage analysis. Summarizing,

$$\beta < \beta_c : \; P_M = P_{reflected}$$

$$\beta > \beta_c : \; P_M = P_{MS},$$

where P_{MS} is the "Mach-stem overpressure," and was obtained from the previously cited tabulations, using the Mach number corresponding to the Mach stem given by

$$M_I = \frac{M_x}{\sin \beta}$$

Where M_x is the Mach number of the incident shock wave.

Figures 4-3 and 4-4 show typical calculations of this type, based on Station 500, and some of the calculations are tabulated in Table 4-2.

4.3.2 Equivalent Static Load Calculation - The equivalent static load method has been described in many references, including Reference 3. The basic principle of the technique is to model the structure as a one-dimensional system characterized by its natural frequency, and to determine a static load that causes the same amount of deformation as the dynamic blast load.

Figure 4-5, obtained from Reference 3, presents equivalent static loads for a ductility ratio of five. The ductility ratio is the ratio of the total deformation at failure to the allowable elastic deformation. A value of 5 for this ratio was found to be consistent with some available experimental data for typical aircraft fuselage structure.

The natural period of the structure must be estimated in order to calculate the equivalent static load. This was done for skin panels, assuming them to be infinitely long and simply supported on each side. The formulas employed were:

$$f = \text{frequency} = 217{,}600\ (0.985)\ \frac{t}{b^2}$$

and,

$$T = \frac{1}{f},$$

where

f = frequency in cycles/second

t = skin thickness

b = panel width, i.e., distance between stiffeners

A typical calculation is shown in Table 4-3.

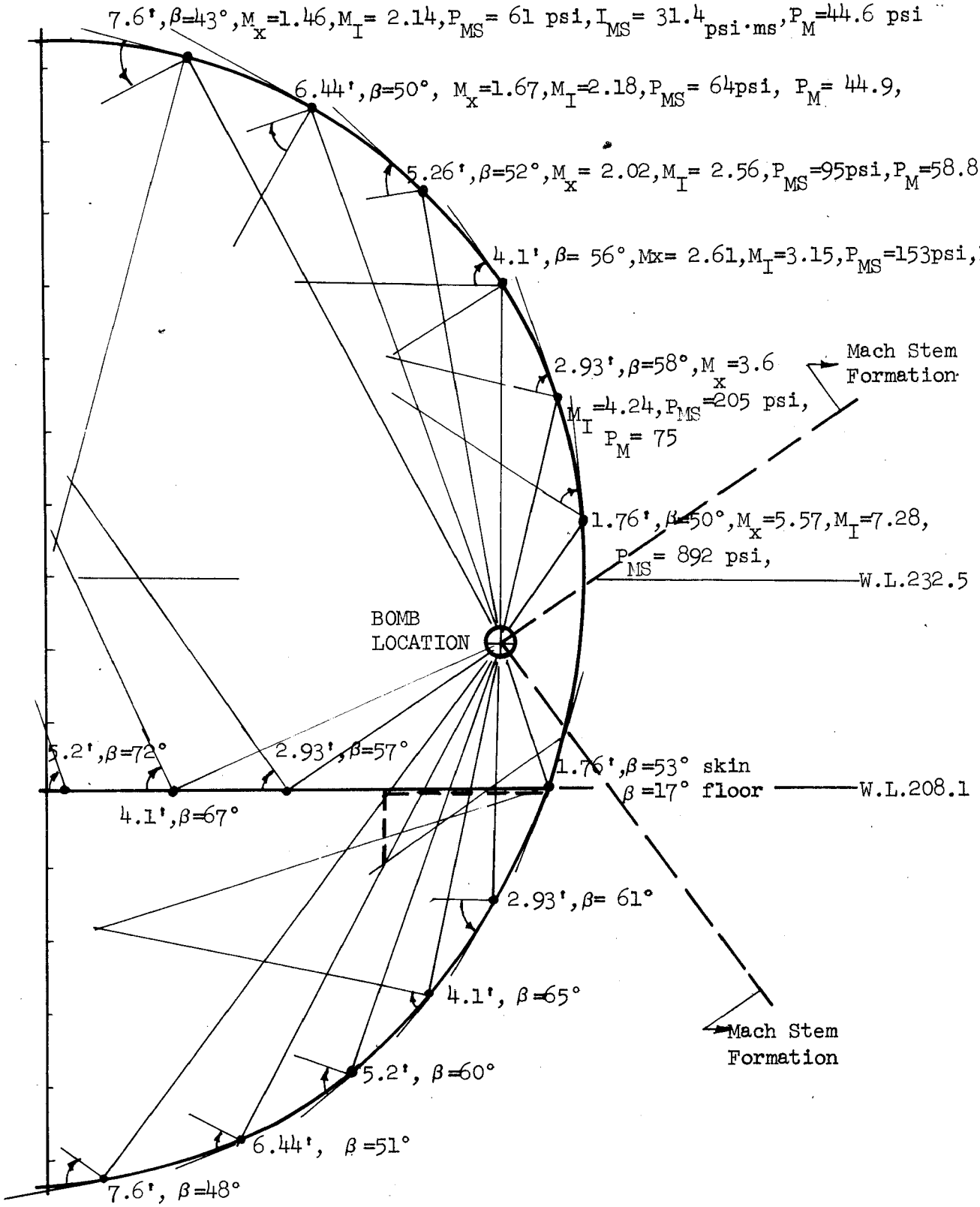

FIGURE 4-3 Calculation of Peak Mach Stem & Reflected Overpressures at Sta.500

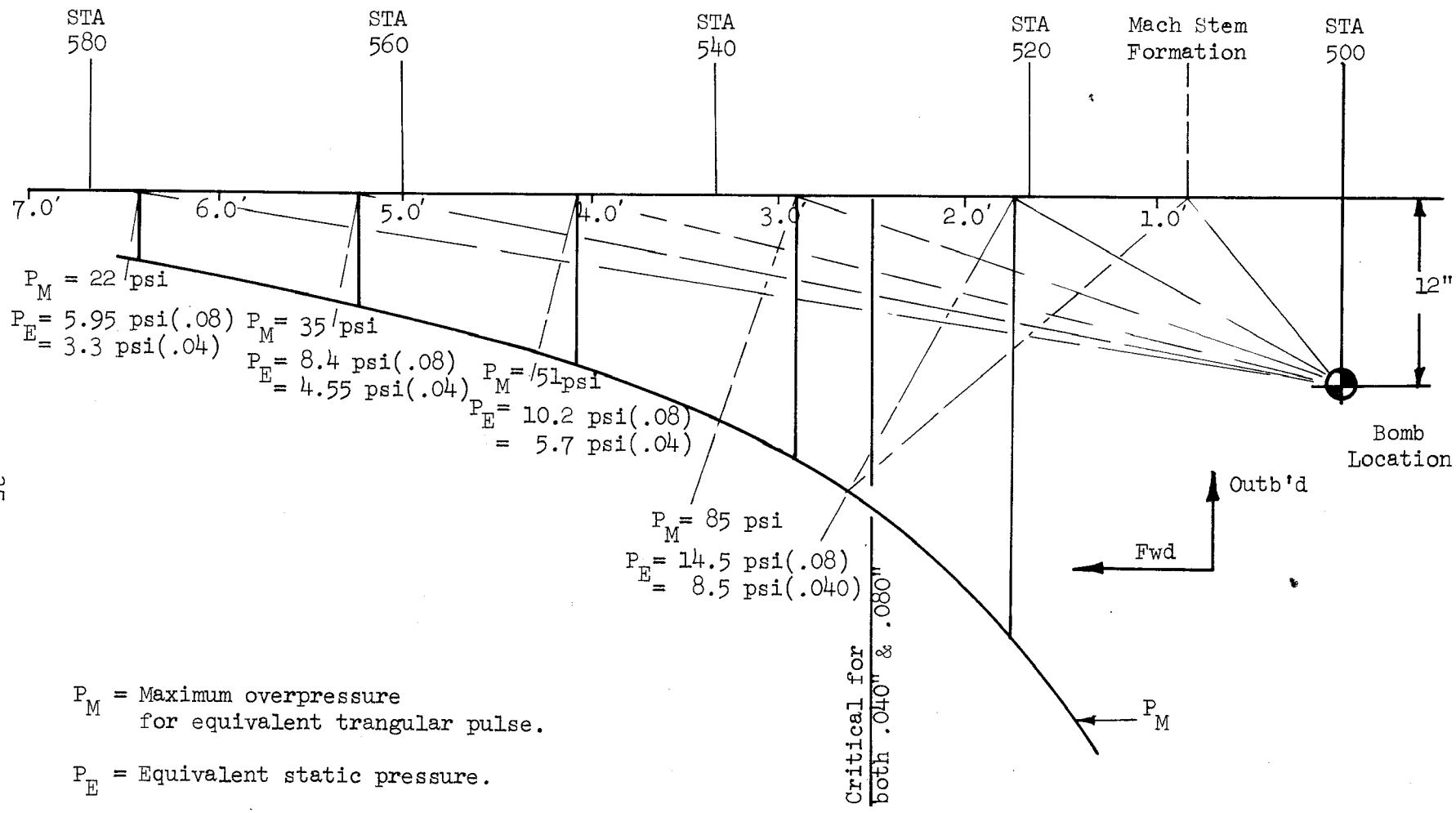

FIGURE 4-4. Mach Stem & Reflected Overpressures

TABLE 4-2 CALCULATIONS FOR MACH STEM PRESSURES (STATION 500 - FORE & AFT)

Distance (ft)	(M_x) Mach No.	β	Mach Stem Mach No. ($M_x/\sin\beta$)	Mach Stem Overpressure	Mach Stem Impulse (psi · ms)	Mach Stem Equiv Triangular Pulse	
						P_{max}	t_d
1.76	5.57	60°	6.43	690			
2.93	3.60	71°	3.81	232	28	85	0.66
4.10	2.61	76°	2.69	107	19.3	51	0.76
5.26	2.02	79°	2.06	56	16.8	35	0.97
6.44	1.67	80°	1.70	32	13.3	22	1.19
7.60	1.46		1.46	19.5	10.0	14	1.41

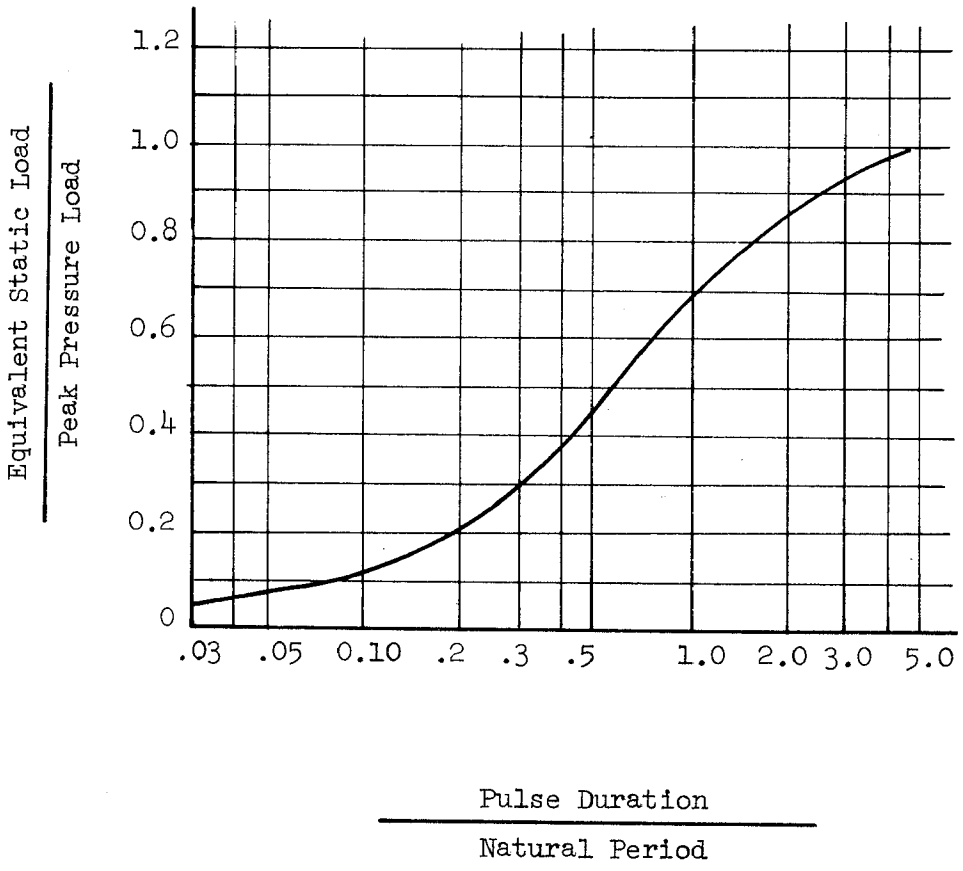

FIGURE 4-5. Equivalent Static Load for Ductility Ratio of 5

TABLE 4-3. EQUIVALENT LOAD CALCULATION

.040 skin, 2024-T3 STA 500 UPPER SKIN

Natural Frequency:

$$f = 217{,}600\ (0.985)\ \frac{t}{b^2}$$

$t = .040$

$b = 8.5"\ (b^2) = (8.5)^2 = 72.2$

$$\therefore \quad f = (217{,}600)(0.985)\left(\frac{.040}{72.2}\right) = 118.5 \text{ cps}$$

$$T = \frac{1}{f} = \frac{1}{118.5} = 8.45 \text{ ms}$$

Distance	t_d (ms)	$t_{d/T}$	$\frac{P_{static}}{P_{max}} = \frac{P_E}{P_M}$
7.6	1.41	0.167	0.175
6.44	1.19	0.141	0.15
5.26	0.97	0.114	0.13
4.10	0.76	0.09	0.11
2.93	0.66	0.078	0.10
1.76			

4.3.3 Failure Calculations - The final step in the structural damage estimation was to use the equivalent static pressure loads to predict failure of skin panels. The skin failure criteria was selected from Reference 3, and is shown in Figure 4-6.

A preliminary calculation indicated that stiffeners would fail in regions of extensive skin failure. In addition, it was assumed that frames would fail within regions of reflected overpressure. Floor failure was estimated in the same manner, using design calculations for sandwich panels. Figures 4-7, 4-8, and 4-9 show minimum and maximum damages in three selected locations.

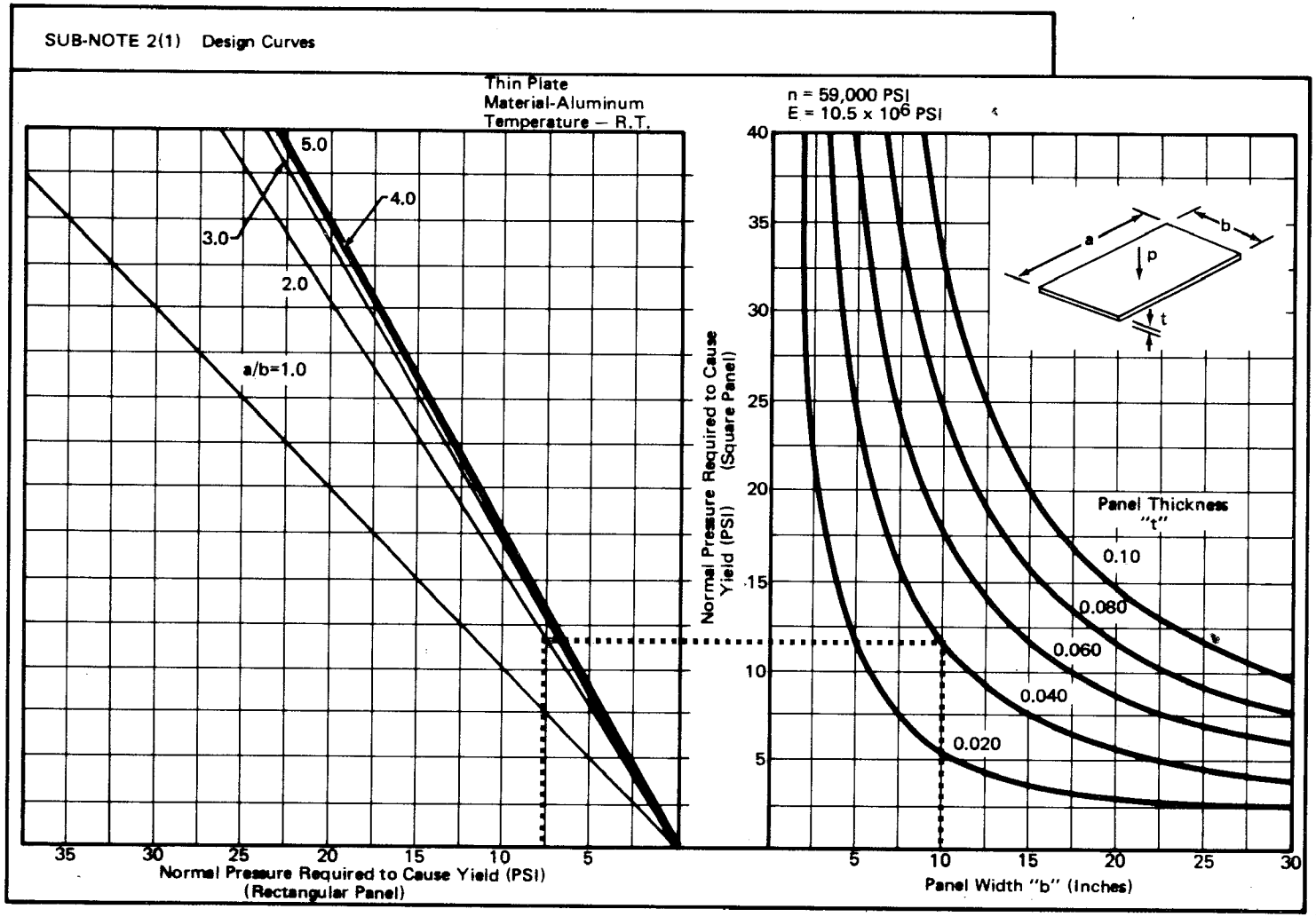

FIGURE 4-6 Skin Failure Criteria